Available online at www.sciencedirect.com
SCIENCE DIRECT®
Ocean Engineering 31 (2004) 2209–2225
OCEAN ENGINEERING
www.elsevier.com/locate/oceaneng

A comparison of sea-state parameters from nautical radar images and buoy data

P. Izquierdo [a], C. Guedes Soares [a,*], J.C. Nieto Borge [b], G.R. Rodríguez [c]

[a] *Unit of Marine Technology and Engineering, Technical University of Lisbon, Instituto Superior Técnico, 1049-001 Lisbon, Portugal*
[b] *German Aerospace Center (DLR), D-82234 Wessling, Germany*
[c] *Department of Physics, University of Las Palmas de Gran Canaria, Campus Universitario de Tafira, 35017 Las Palmas de Gran Canaria, Spain*

Received 31 October 2003; accepted 23 April 2004

Abstract

Nautical radar and scalar buoy measurements of ocean wind generated waves have been analysed to compare the spectral parameters estimated from both sensors. The time series of different sea-state parameters and the differences and ratios of the values obtained from radar and buoy data using different analysis methods are compared. It has been observed that main differences between the sea-state parameters derived by using measurements obtained from both sensors result both from device characteristics and from the method of spectral estimation. In particular, it is shown that the Nyquist frequency has an important effect on the value of the sea-state parameters depending on spectral moments of order higher than zero.

Keywords: Sea-state parameters; Ocean waves; Nautical radar and scalar buoy

1. Introduction

Methodologies that enable the extraction of useful information about ocean wave fields from conventional nautical radars have been developed during the last two decades. In particular, it is possible to estimate the directional wave spectrum and the related spectral sea-state parameters by using a temporal sequence of radar images of the sea surface, thus containing information about the spatial and temporal dependence of sea states. On the other hand, buoys are the traditional

* Corresponding author. Tel.: +351-218-417-607; fax: +351-218-474-015.
E-mail address: guedess@mar.ist.utl.pt (P. Izquierdo).

0029-8018/$ - see front matter © 2004 Elsevier Ltd. All rights reserved.
doi:10.1016/j.oceaneng.2004.04.004

devices used to record time series of sea surface elevation providing information at a fixed point in space.

Comparison of results obtained by spectral analysis of measurements gathered with so different sensors, such as scalar buoys and a nautical radars, should be accompanied of some statistical assessment of the agreement between the sea-state parameters estimated from each one. Some comparisons between nautical radar image time series and scalar wave data (Alfonso et al., 1997; Nieto Borge and Guedes Soares, 2000) and also directional Waverider buoy data (Nieto Borge et al., 2000) have been recently developed. However, in these studies, comparisons of sea-state parameters have been presented basically in an illustrative way but no statistics were calculated to quantify the degree of agreement between the parameters estimated from the data sets provided by the different sensors, as suggested by Krogstad et al. (1999).

In the present work, the spectral sea-state parameters derived by analysing time series of nautical radar images are compared with those estimated by means of spectral analysis of wave records registered simultaneously by using a conventional scalar buoy placed in the same location. Temporal evolution of different sea-state parameters, as well as some statistics of the differences and ratios between parameters estimated from radar and buoy measurements are presented.

2. Data set

The data set analysed was collected during the calibration period of a nautical radar station located on the northern coast of Spain (Cabo de Peñas), from 28 February to 23 April 2000. The data set consists of 312 time series of nautical radar images and the same number of sea surface elevation records simultaneously gathered. The scalar Waverider buoy was moored close to the area covered by the radar. Fig. 1 shows the locations of the buoy and the radar in Cabo de Peñas.

During this period, the radar measured each hour 12 radar image time series. The temporal separation between radar image time series was 2.5 min. Each radar image time series is composed of 32 consecutive images with the sampling time given by the antenna rotation period (1.84 s). The imaged sea surface area used for spectral analysis was of 128×256 pixels in the north and east directions, respectively, with an image resolution in both directions of 9.091×9.091 squared meters per pixel.

The scalar buoy used was a Datawell Waverider model. The buoy recorded each hour during a period of 17 min, a time series composed of 2048 points with a sampling interval of 0.5 s.

3. Spectral analysis of data

3.1. Analysis of radar image time series

Nautical radar images of the sea surface are not a direct mapping of the sea surface elevation because these radar images are affected by all those phenomena

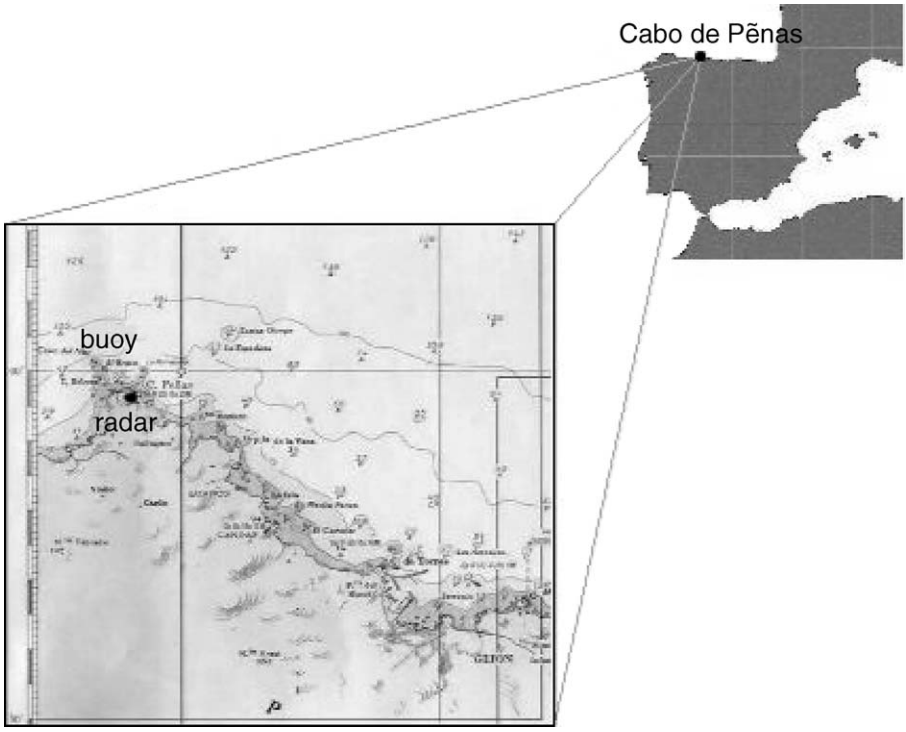

Fig. 1. Locations of the radar station and the scalar buoy in Cabo de Peñas.

responsible of the backscattering of the electromagnetic fields emitted by the radar antenna. The backscatter phenomenon is a combination of all those effects, which produce changes in the local roughness of the sea surface, such as the local wind, hydrodynamic modulations, wave tilting, etc. Hence to extract wave field information from radar images an inverse modelling technique is needed, which filter out all those phenomena presented in the radar image that are not related to the wave field elevation. The inversion procedure used to estimate the wave spectral density from a radar image time series consists of applying a three-dimensional Fourier transform (3D-FFT) to compute a three-dimensional image spectrum, $F_{\psi}^{(3)}(\vec{k},\omega)$, in wave number vector, $\vec{k}=(k_x,k_y)$, and angular frequency, ω, domains (Young et al., 1985). The energy associated with the ocean waves is extracted from the image spectrum by previously estimating the surface current (Senet et al., 1997) and applying the dispersion relation as a band-pass filter (Young et al., 1985; Seemann et al., 1997). Then, the image spectrum values are related to wave spectrum values using a transfer function (Nieto Borge et al., 1999). More details about the inversion method are given by Nieto Borge and Guedes Soares (2000).

The series of 32 consecutive images were analysed by the WaMoS II system (Nieto Borge et al., 1999) to estimate the ocean wave spectrum in the frequency

domain, $S(f)$, with a frequency resolution of 0.0045 Hz and a Nyquist frequency of 0.288 Hz. The average of spectra from 12 image series registered each hour was performed to obtain a smoother spectrum with 48 degrees of freedom (d.o.f.).

3.2. Analysis of scalar wave buoy

The time series of sea surface elevation registered by the scalar buoy were analysed using the classic method of one-dimensional fast Fourier transform (1D-FFT) to estimate the ocean wave spectrum in the frequency domain. The spectra were smoothed by means of the Daniell's, Bartlett's and Welch's methods (Rodríguez, 1993). To compare their results with those from the radar, these spectral methods were chosen because they are based on the use of the fast Fourier transform algorithm, as in the procedure used for the spectral analysis of radar image time series.

In Daniell's method, the analysis consisted on the application of 1D-FFT algorithm to the time series of surface elevation, obtaining the discrete estimations of the frequency spectrum, $S(f)$. The spectra were smoothed performing an average of 13 spectral estimations at consecutive frequencies obtaining spectra with 26 d.o.f. These spectra have a frequency resolution of 0.0127 Hz and a Nyquist frequency of 0.1 Hz.

In Bartlett's method, each time series was divided in 12 consecutive segments of 128 data points of sea surface elevation from which the frequency spectrum was calculated by applying a 1D-FFT algorithm. The averaging of spectra was performed resulting in a smoothed spectrum of 24 d.o.f. with a frequency resolution of 0.0156 Hz and a Nyquist frequency of 0.1 Hz.

To apply the Welch's procedure, each time series of sea surface elevation was divided into 12 overlapping segments of 128 data points with a 25% ratio of overlapping. A taper cosine window was applied to each of the segments to reduce leakage effects. A 1D-FFT algorithm was run on each segment to estimate their raw spectra. Finally, the 12 raw spectra were averaged to obtain a smoothed spectrum with 24 d.o.f. The spectra estimated with this procedure have a frequency resolution of 0.0156 Hz and a Nyquist frequency of 0.1 Hz.

3.3. Radar calibration

The spectra, obtained from the radar after the inversion method described, has values that are related to the scale of sampled grey levels of the radar image time series, containing only relative information about the energy distribution of the wave field. Hence, these non-scaled spectra cannot provide the variance of the sea surface elevation, $\eta(\vec{r}, t)$, nor the related parameters such as the spectral zero-order moment, m_0, or the significant wave height, H_S. Therefore, to obtain the real spectral values corresponding to the sea state, each nautical radar station needs to go through a calibration process.

This radar was calibrated using this set of 312 simultaneous observations from the radar and the buoy. It was made by the method developed for the Synthetic Aperture Radar (Alpers and Hasselmann, 1982), which is based on the assumption that the square-root of signal to noise ratio SNR of radar measures is linearly

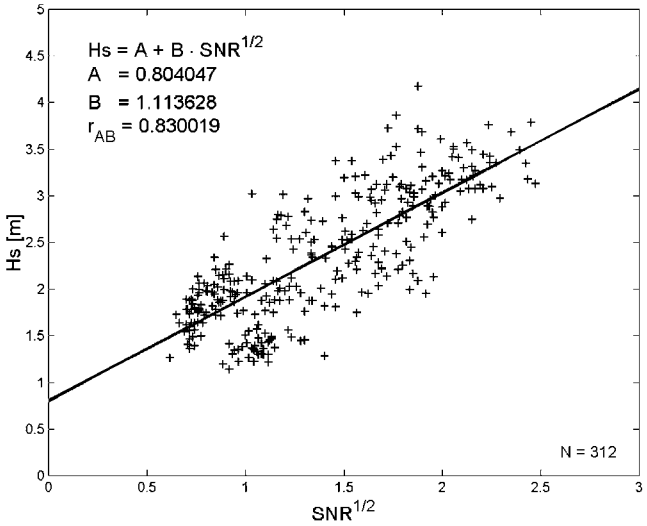

Fig. 2. Linear least-square fit of H_S versus $SNR^{1/2}$.

related to significant wave height H_S. For this aim, the mean values of the SNR from each 12 radar image series measured per hour and the values of the H_S estimated from buoy series by Daniell's method were used to calibrate the radar station. In Fig. 2, the linear regression of the calibration is shown.

4. Spectral parameters of sea state

To compare the spectral parameters derived from the scalar buoy and the nautical radar measurements, they were estimated from the frequency spectra, $S(f)$, computed from both sensors. The parameters examined are the significant wave height, peak frequency, mean period, spectral maximum and spectral bandwidth. The differences and ratios of the values of these parameters obtained from both devices were also calculated.

The data used for the radar calibration was the same as the data used in the comparison of spectral parameters. That is important to be taken into account in the comparison of the significant wave height from both sensors because the values of this parameter estimated from the buoy data were used to calibrate the radar. Then, the significant wave height from both sensors is expected to have no bias, but the variability around the mean regression and the values of other spectral parameters studied in this work are independent of the radar calibration.

It is worth of mention that in the comparison of the sea-state parameters estimated from radar and buoy measurements, the different nature of the data has to be taken into account. The radar records time series of images in an area of the sea surface whereas the buoy records time series of free surface elevation at a point. Because of this, the parameters resulting of the spectral analysis of the radar measurements represent mean values in space and time while those derived from the

buoy only includes temporal information. Therefore, it is obvious that, even in the hypothetical case that both sensors could measure the sea surface elevation with the same resolution and work with equivalent sampling period and recording period, the spatial information provided by the radar will lead to differences in the estimated spectral densities in relation to that obtained from the buoy, except in the case of a spatially homogeneous sea surface.

The sampling periods of the sensors used in this study are also very different, 0.5 s for the buoy and 1.58 s for the radar. As a consequence, the Nyquist frequency, f_N, associated to the measurements of both sensors are also different.

To examine the effects of the Nyquist frequency on the on the sea-state parameters estimated from the overall spectral density, the parameters derived from the buoy wave records have been estimated in two ways, integrating the spectral density up to its associated Nyquist frequency (1 Hz), and integrating it only up to the Nyquist frequency of the radar spectra (0.27 Hz).

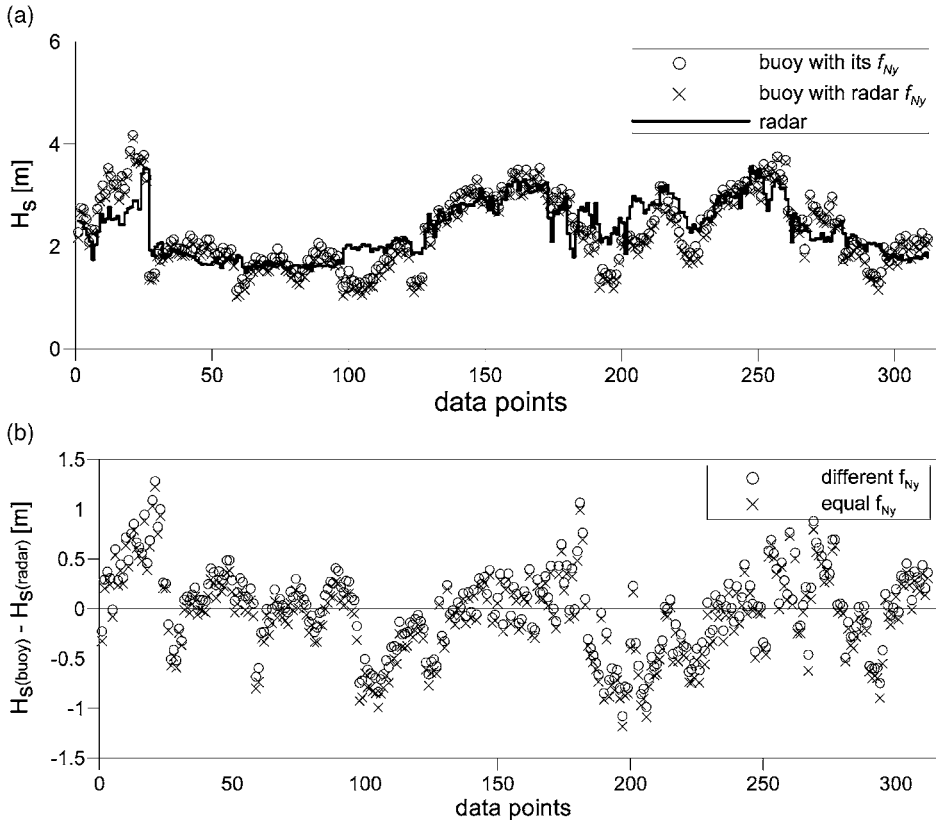

Fig. 3. Values of H_S from the radar and the buoy, (a), and their differences $H_S(\text{buoy}) - H_S(\text{radar})$, (b).

4.1. Significant wave height

The significant wave height, H_S, was calculated from buoy and radar frequency spectra assuming that the wave height follows the Rayleigh distribution. Consequently, it can be expressed as

$$H_S = 4\sqrt{\int_0^{f_N} S(f)\mathrm{d}f} \tag{1}$$

Fig. 3 shows time series of H_S estimated from radar and from buoy spectra, the last one estimated with Daniell's method, and of the differences between these values calculated from both sensors, $H_{Sbuoy} - H_{Sradar}$. In general, the values of the significant wave height estimated by using radar and buoy data presented similar behaviour. Nevertheless, the time series of the radar had an evolution smoother than those of the buoy due to the fact that estimation procedure of this parameter from radar data integrates spatial and time information while in the case of a scalar buoy only temporal information is considered. So, mean values in space and time (radar estimations) are compared versus mean values in time (buoy estimations).

4.2. Peak frequency

The peak frequency, f_p, was calculated by Delft's method defined by the IAHR working group (IAHR, 1989) as

$$f_p = \frac{\int_{f_1}^{f_2} fS(f)\mathrm{d}f}{\int_{f_1}^{f_2} S(f)\mathrm{d}f} \tag{2}$$

where f_1 and f_2 are the lowest and the highest frequencies of the range $S(f) \geq 0.8 \max\{S(f)\}$, respectively. Fig. 4 shows the time series of f_p estimated from radar and from buoy spectra, the last one is estimated with Daniell's method and of the differences between these values calculated from both sensors, $f_{pbuoy} - f_{pradar}$.

The peak frequency was the parameter that presented the highest similarity between buoy and radar estimations. The few cases in which this parameter presented different values in the two series were when the sea state was a combined wave field of swell and wind–sea. One can see in Fig. 4 the ranges of data points [46,68] and [86,96] in which discrepancies have occurred. Figs. 5 and 6 show two typical cases of those discrepancies. In the first one, the radar detected the wind–sea but with less energy than the radar. On the second case the radar did not detected the wind–sea component.

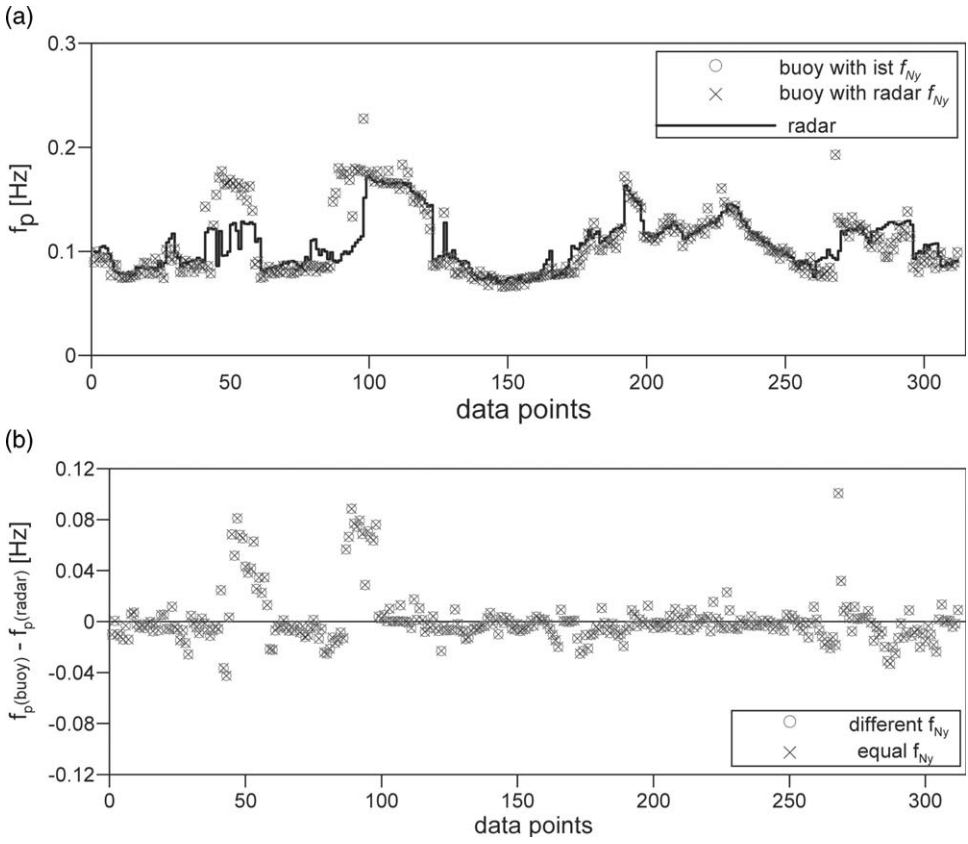

Fig. 4. Values of f_p from the radar and the buoy, (a), and their differences $f_p(\text{buoy}) - f_p(\text{radar})$, (b).

4.3. Mean period

The values of mean period, $\bar{T}$, were calculated according to the theory of random waves defined (Rice, 1944) as

$$\bar{T} = \sqrt{\frac{\int_0^{f_N} S(f)\mathrm{d}f}{\int_0^{f_N} f^2 S(f)\mathrm{d}f}} \tag{3}$$

Fig. 7 shows the time series of $\bar{T}$ estimated from radar and buoy spectra estimated with Daniell's method and of differences between these values calculated from both sensors, $\bar{T}_{\text{buoy}} - \bar{T}_{\text{radar}}$. The values of mean period estimated by using buoy data were lower than those derived from the radar. This is due to the dependence of this parameter on the second order spectral moment. Bearing in mind that the spectral moments of higher order enhance the spectral energy at high frequencies, the

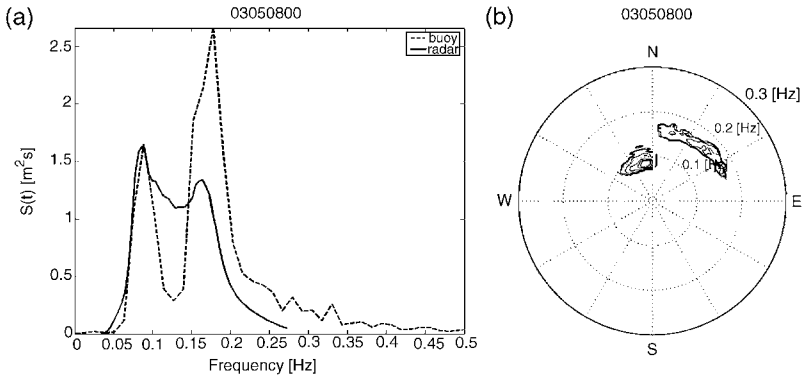

Fig. 5. Spectra corresponding to data point 46: (a) frequency spectra from radar and buoy data; and (b) spectrum in frequency and direction from radar data.

energy of buoy spectra located in frequencies higher than the Nyquist frequency of the radar gives rise to a lower estimated mean period from buoy data in comparison with that from the radar data.

When this parameter was estimated from buoy spectra by integrating the spectrum energy only up to the Nyquist frequency of the radar spectra, the values were very close to the ones estimated from radar spectra except during the period of data points [38, 130] in Fig. 6 where the buoy estimations were lower. This was because the spectral energy of the buoy was less than the one from radar at the high frequencies up to the Nyquist frequency of radar spectra. This situation happened in the period in which bimodal wave fields were recorded (see Figs. 5, 6 and 8).

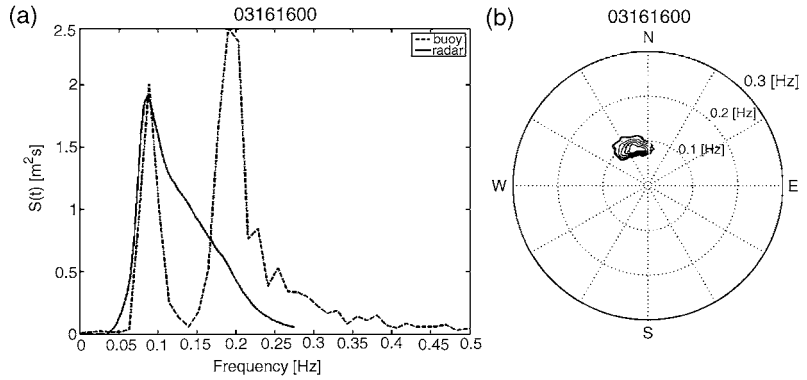

Fig. 6. Spectra corresponding to data point 87: (a) frequency spectra from radar and buoy data; and (b) spectrum in frequency and direction from radar data.

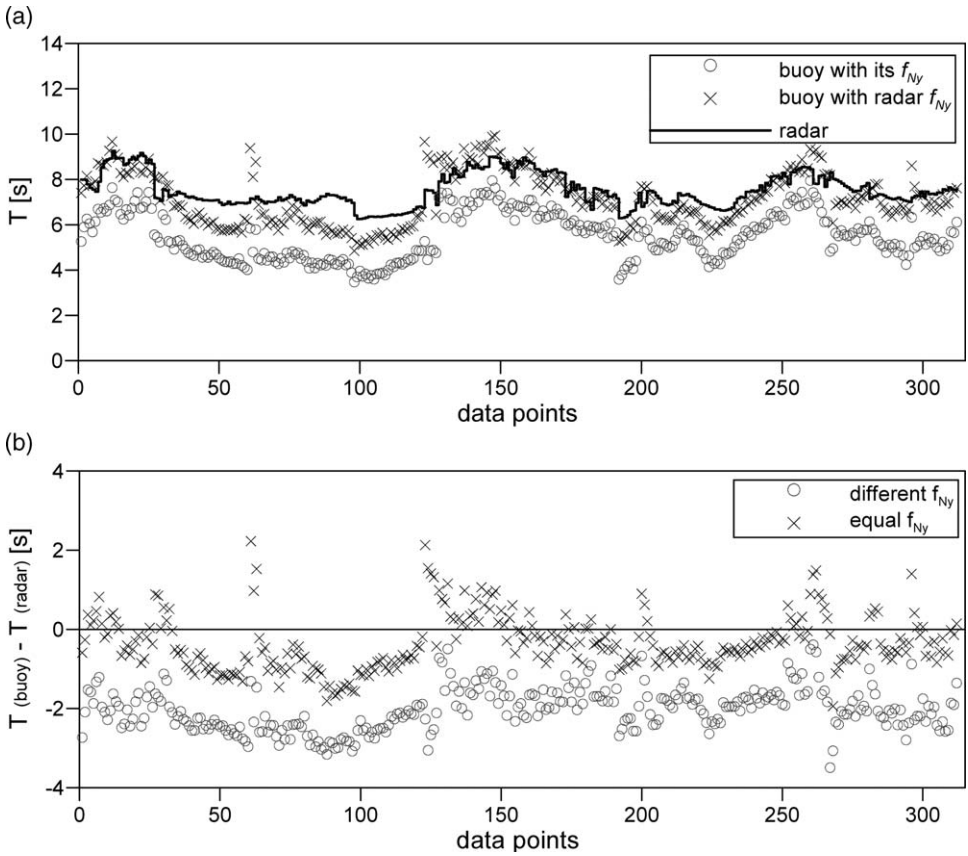

Fig. 7. Values of $\bar{T}$ from the radar and the buoy, (a), and their differences $\bar{T}(\text{buoy}) - \bar{T}(\text{radar})$, (b).

4.4. Spectral maximum

The spectral maximum

$$\max\{S(f)\} = S(f_{\text{p}}) \tag{4}$$

was the parameter that presented the largest differences between the estimations from radar and buoy.

Fig. 9 shows time series of spectral maximum, $\max\{S(f)\}$, estimated from radar and from buoy spectra estimated with Daniell's method and of differences between these values calculated from both sensors, $\max\{S(f)\}_{\text{buoy}} - \max\{S(f)\}_{\text{radar}}$.

The large differences in spectral maximum result from the fact that the spectra $S(f)$ estimated with the radars have smoother forms. This is due to smaller frequency resolution than those from the buoy and radar spectra are resulting of the integration in space of the three-dimensional spectrum. The smoother form of the

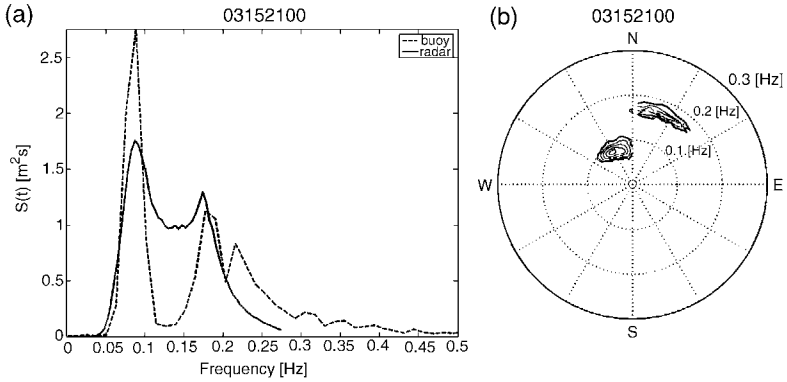

Fig. 8. Spectra corresponding to data point 69: (a) frequency spectra from radar and buoy data; and (b) spectrum in frequency and direction from radar data.

radar spectra had as a consequence that in most cases the values of spectral maximum estimated by buoy were higher than those by radar.

4.5. Spectrum bandwidth

The spectral bandwidth, v, defined by Longuet-Higgins (1975), was adopted in this work

$$v = \sqrt{\frac{\int_0^{f_N} S(f)\mathrm{d}f \int_0^{f_N} f^2 S(f)\mathrm{d}f}{\left[\int_0^{f_N} fS(f)\mathrm{d}f\right]^2}} \tag{5}$$

This parameter has values between 0 and 1. When $v \leq 0.1$, the spectrum bandwidth is infinitesimal, when $v \leq 0.5$ it is narrow and when $v > 0.5$ it is wide (Rodríguez, 1995). Fig. 10 shows time series of v from radar and from buoy spectra, the last ones estimated with Daniell's method and of differences between these values calculated from both sensors, $v_{\mathrm{buoy}} - v_{\mathrm{radar}}$.

The values of the spectral bandwidth estimated by the radar were smaller than those of the buoy. This parameter depends on the spectral moments of zeroth, first and second order and, as explained for the mean period, the moments of order greater than zero augment the weight of energy at higher frequencies. The energy of the buoy spectra situated at frequencies between the radar and the buoy Nyquist frequency originates that effect.

When this parameter was estimated from buoy spectra by integrating the spectrum energy as far as the Nyquist frequency of radar spectra, the values were similar to those estimated from radar spectra (see Fig. 10). This is because radar measurements underestimate the high frequency contribution to the higher order moments as compared with buoys.

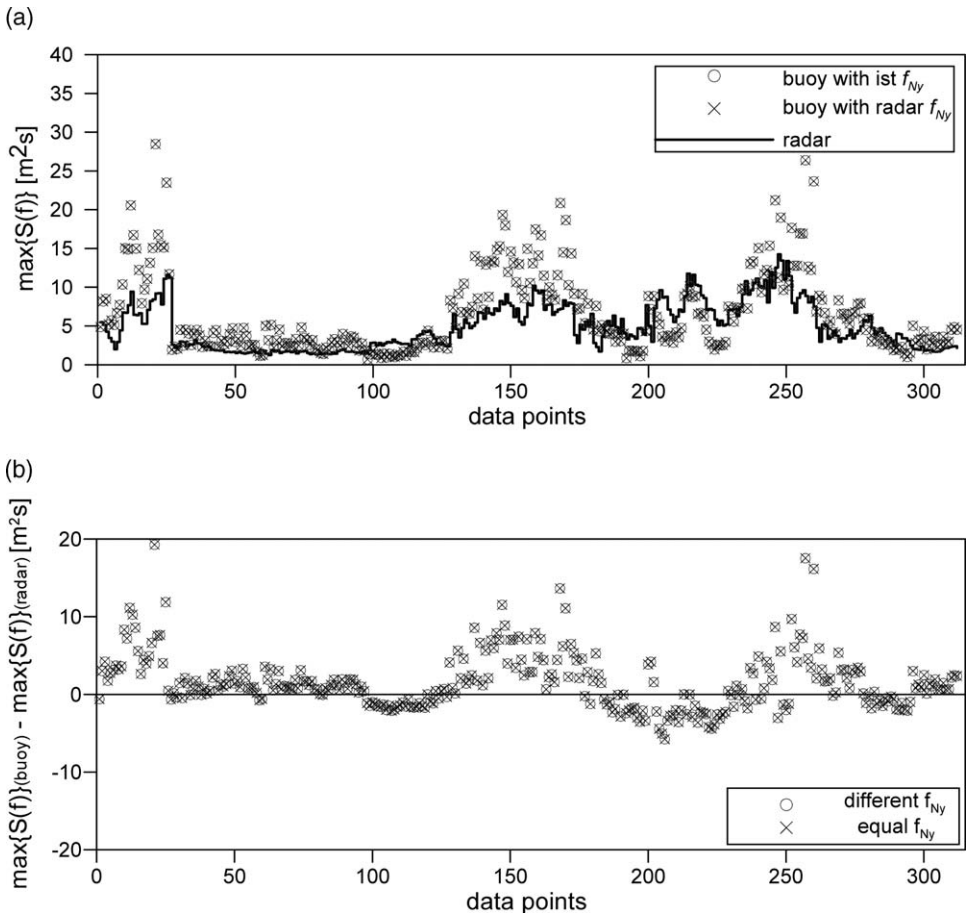

Fig. 9. Values of max $\{S(f)\}$ from the radar and the buoy, (a), and their differences $\max\{S(f)\}(\text{buoy}) - \max\{S(f)\}(\text{radar})$, (b).

5. Statistics of parameters

To make a quantitative comparison between the sea-state parameters estimated from buoy and radar data, the mean and standard deviation of the differences and the ratios of each parameter were estimated. The results are shown in Tables 1, 2 and 3, respectively, for Daniell's, Bartlett's and Welch's spectral method used on the buoy data.

The significant wave height was in general similar, independent of spectral method used for the buoy data, having means of 0.00 and 1 m, respectively, for the differences and ratios of buoy and radar values. The values of the differences estimated from buoy spectra as far as the Nyquist frequency of radar spectra, were a little low having small repercussion in the statistics.

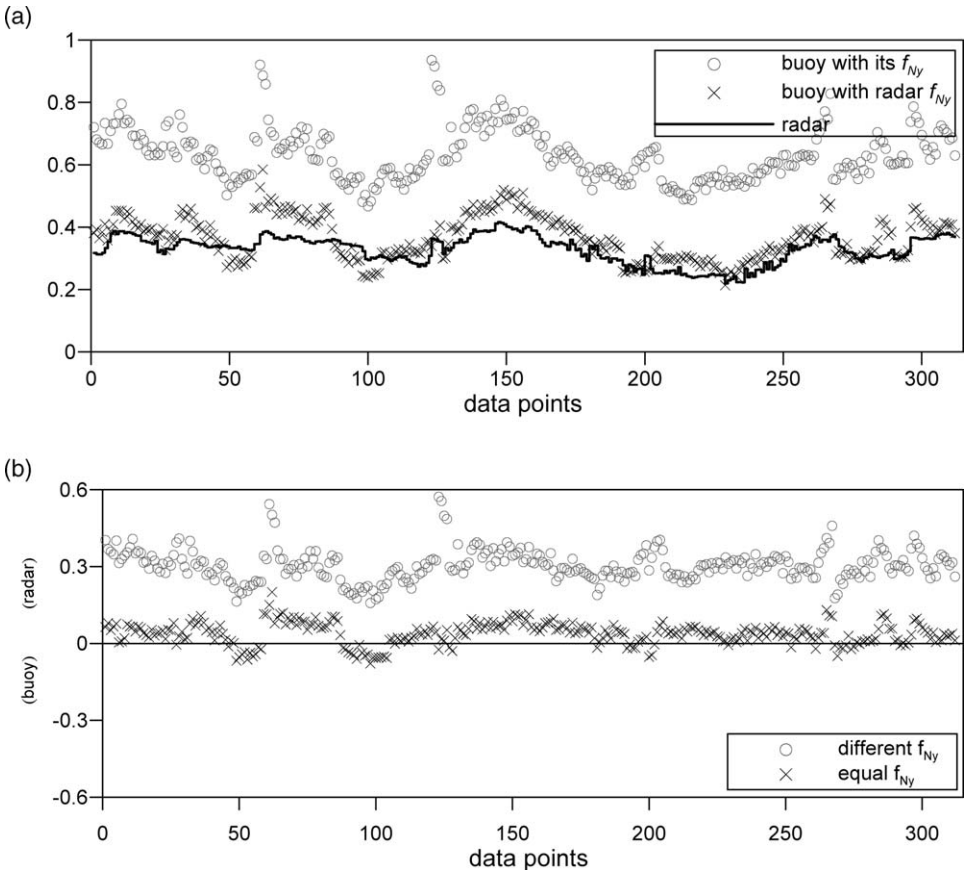

Fig. 10. Values of v from the radar and the buoy, (a), and their differences v(buoy)/v(radar), (b).

The peak frequency had very similar estimations from radar and buoy spectra. This is reflected in the means of their differences and ratios being 0 and 1 Hz, respectively, for all spectral methods applied to buoy data and for the frequency range used in their estimations equal to that of radar spectra.

Usually, the mean period was lower from the buoy due to the energy of buoy spectra located in frequencies higher than Nyquist frequency of radar spectra. As a consequence, the means of differences and ratios between estimations from buoy and radar was, respectively, around –2 and 0.7 s, but when this parameter was estimated from buoy spectra with the same frequency range as that of radar spectra, the means for differences and ratios were closer to 0 and 1.

The values of spectral maximum estimated from buoy had, in most cases, higher values than those from radar spectra independently of frequency range used in the buoy spectra. This is reflected in the means of the differences and ratios between buoy and radar estimations that are more pronounced in the spectral analysis of

Table 1
Statistics of sea-state parameters from radar and buoy data analysed with Daniell's method

	$f_{Ny}(\text{buoy}) \neq f_{Ny}(\text{radar})$		$f_{Ny}(\text{buoy}) = f_{Ny}(\text{radar})$	
	Mean	rms	Mean	rms
$H_S(\text{buoy}) - H_S(\text{radar})$	0.00	0.41	−0.09	0.42
$f_p(\text{buoy}) - f_p(\text{radar})$	0.00	0.02	0.00	0.02
$\bar{T}(\text{buoy}) - \bar{T}(\text{radar})$	−2.02	0.54	−0.35	0.68
$\max\{S(f)\}(\text{buoy}) - \max\{S(f)\}(\text{radar})$	1.61	3.58	1.61	3.58
$\nu(\text{buoy}) - \nu(\text{radar})$	0.30	0.06	0.04	0.04
$H_S(\text{buoy})/H_S(\text{radar})$	1.00	0.18	0.96	0.19
$f_p(\text{buoy})/f_p(\text{radar})$	1.01	0.20	1.01	0.20
$\bar{T}(\text{buoy})/\bar{T}(\text{radar})$	0.73	0.08	0.95	0.09
$\max\{S(f)\}(\text{buoy})/\max\{S(f)\}(\text{radar})$	1.38	0.68	1.38	0.68
$\nu(\text{buoy})/\nu(\text{radar})$	1.95	0.22	1.11	0.13

Table 2
Statistics of sea-state parameters from radar and buoy data analysed with Bartlett's method

	$f_{Ny}(\text{buoy}) \neq f_{Ny}(\text{radar})$		$f_{Ny}(\text{buoy}) = f_{Ny}(\text{radar})$	
	Mean	rms	Mean	rms
$H_S(\text{buoy}) - H_S(\text{radar})$	0.00	0.41	−0.10	0.42
$f_p(\text{buoy}) - f_p(\text{radar})$	0.00	0.02	0.00	0.02
$\bar{T}(\text{buoy}) - \bar{T}(\text{radar})$	−2.26	0.48	−0.42	0.67
$\max\{S(f)\}(\text{buoy}) - \max\{S(f)\}(\text{radar})$	0.64	2.78	0.64	2.78
$\nu(\text{buoy}) - \nu(\text{radar})$	0.35	0.07	0.05	0.04
$H_S(\text{buoy})/H_S(\text{radar})$	1.00	0.18	0.95	0.19
$f_p(\text{buoy})/f_p(\text{radar})$	1.02	0.20	1.02	0.20
$\bar{T}(\text{buoy})/\bar{T}(\text{radar})$	0.70	0.08	0.94	0.09
$\max\{S(f)\}(\text{buoy})/\max\{S(f)\}(\text{radar})$	1.19	0.58	1.19	0.68
$\nu(\text{buoy})/\nu(\text{radar})$	2.09	0.24	1.16	0.13

Table 3
Statistics of sea-state parameters from radar and buoy data analysed with Welch's method

	$f_{Ny}(\text{buoy}) \neq f_{Ny}(\text{radar})$		$f_{Ny}(\text{buoy}) = f_{Ny}(\text{radar})$	
	Mean	rms	Mean	rms
$H_S(\text{buoy}) - H_S(\text{radar})$	0.00	0.41	−0.12	0.42
$f_p(\text{buoy}) - f_p(\text{radar})$	0.00	0.02	0.00	0.02
$\bar{T}(\text{buoy}) - \bar{T}(\text{radar})$	−2.25	0.48	−0.28	0.69
$\max\{S(f)\}(\text{buoy}) - \max\{S(f)\}(\text{radar})$	0.63	2.78	0.63	2.78
$\nu(\text{buoy}) - \nu(\text{radar})$	0.35	0.07	0.04	0.04
$H_S(\text{buoy})/H_S(\text{radar})$	1.00	0.18	0.95	0.19
$f_p(\text{buoy})/f_p(\text{radar})$	1.02	0.20	1.02	0.20
$\bar{T}(\text{buoy})/\bar{T}(\text{radar})$	0.70	0.08	0.96	0.09
$\max\{S(f)\}(\text{buoy})/\max\{S(f)\}(\text{radar})$	1.19	0.58	1.19	0.58
$\nu(\text{buoy})/\nu(\text{radar})$	2.08	0.23	1.12	0.13

buoy data with Daniell's method due to less effective smoothing of this method. The standard deviations of differences and ratios were high because this parameter was the one which presented more divergences between the estimations from both sensors.

The spectral bandwidth always had values estimated from buoy higher than those from radar spectra. Because of this, the differences and ratios between buoy and radar values were around 0.3 and 2, respectively. When the estimations from buoy spectra were made using the spectral energy located in frequencies as far as Nyquist frequency of radar spectra, these values were very close to the radar values implying the means of differences and ratios were brought near to 0 and 1, respectively. This is due to the energy of buoy spectra, located in frequencies higher than Nyquist frequency of radar spectra, being significant when calculating higher order spectral moments.

The statistics of the main sea-state parameters showed similar values indicating that on the average over the long term the instruments provide the same type of climatic information. However, there is some variability which can lead in individual cases to differences of ± 1 m in significant wave height and ± 1.5 s in mean period. It was found that the largest discrepancies occurred in combined sea states of sea–wind and swell indicating that the performance of the instruments in this case needs to be better studied.

6. Conclusions

A comparative analysis of sea-state parameters estimated from nautical radar and Waverider buoy measurements in Cabo de Peñas was made in the present work. The time series of significant wave height, peak frequency, mean period, spectral maximum and spectral bandwidth as well as means and standard deviations of the differences and ratios between values estimated from both sensors were shown.

The time series of the simultaneous sea-state parameters from both sensors exhibited a similar trend although radar's data were smoother than the buoy's. This is due to the frequency spectra estimated from the radar being obtained by the integration in wave number of the three-dimensional spectrum. Because of this, the estimation that is obtained for the spectrum contains both temporal and spatial information of the wave field while, for case of the buoy, only temporal information at a given point is taken into account.

The Nyquist frequencies from both types of sensors are not the same and this originates different values for the spectral moments of order higher than zero. Because the Nyquist frequency of the radar is lower than that of the buoy, the energy of buoy spectra, located at frequencies higher than Nyquist frequency of radar spectra, has its weight augmented as the order of spectral moment increase, leading to larger mean periods to be estimated from the radar and larger bandwidth from the buoy. However, taking into account the same frequency range of

radar and buoy spectra, the values of sea-state parameters studied from both sensors were more similar.

The mean errors for significant wave height and peak frequency are very small, demonstrating the long-term reliability of this equipment for monitoring these parameters. The comparison of mean and spectral bandwidth period shows additionally that whenever an appropriate Nyquist frequency can be ensured for the radar the estimations of mean period agree well with the ones from buoy. Considering now the variability of the estimates, one can observe relatively high values of 40% for significant wave height deviation although only 20% for the ratio of observation. It is interesting to note that the opposite variation happens with the statistics of peak frequency, which show a very small variability of 2% for the differences but this increases so about 20% for the ratio of frequencies. This observation of the different tendencies in the evolution of the statistics of errors show that it is useful to use both definitions in order to have a better description of how the parameter statistics evolve.

In order to provide a better basis to interpret the values of the statistics of differences between the observations, Tables 1–3 have been provided so that one can quantify what the uncertainties are just in the estimation of parameters from only buoy data. Comparing the statistics from the three tables is a way of comparing the three methods of estimation of the scalar spectrum from wave time series: Daniel, Barlelt and Welch. The significant wave height and peak period, which are, the two main parameters of the sea state show very small differences for the various estimations. More visible differences can be observed for mean period and spectral bandwidth although these differences become small when the same Nyquist frequency limit is used. These values of uncertainty in the estimation of spectral parameters resulting from the method of estimations are generally in agreement with earlier work in the subject (Rodriguez et al., 1999).

Acknowledgements

This work has been performed within the RADSEANET project (EUREKA-EUROMAR E1893) that was financed by national programs in Portugal and Spain.

The data was collected by Clima Marítimo, Puertos del Estado (Spain) as basis for the calibration of the system to be used in a field experiment under the project EuroROSE that has been partially financed by the European Union through its MAST Programme under contract CT98-0168.

References

Alfonso, M., Muñoyerro, A., Nieto Borge, J.C., 1997. Directional wave navigation radar measurements compared with pitch-roll buoy data. Journal of Offshore Mechanics and Arctic Engineering 119 (1), 25–29.

Alpers, W., Hasselmann, K., 1982. Spectral signal to clutter and thermal noise properties of ocean wave imaging synthetic aperture radars. International Journal of Remote Sensing 3, 423–446.

IAHR working group on wave generation and analysis, 1989. List of sea state parameters. Journal of Waterway, Port, Coastal and Ocean Engineering 115 (6), 793–808.

Krogstad, H.E., Wolf, J., Thompson, S.P., Wyatt, L.R., 1999. Methods for intercomparison of wave measurements. Coastal Engineering 37, 235–257.

Longuet-Higgins, M.S., 1975. On the joint distribution of the periods and amplitudes of sea waves. Journal of Geophysical Research 18 (80), 2688–2694.

Nieto Borge, J.C., Guedes Soares, C., 2000. Analysis of directional wave fields using X-band navigation radar. Coastal Engineering 40, 375–391.

Nieto Borge, J.C., Reichert, K., Dittmer, J., 1999. Use of nautical radar as a wave monitoring instrument. Coastal Engineering 37, 331–342.

Nieto Borge, J.C., Sanz González, R., Hessner, K., Reichert, K., Guedes Soares, C., 2000. Estimation of sea state directional spectra by using marine radar imaging of sea surface. In: Proceedings of the 19th International Conference on Offshore Mechanics and Arctic Engineering, (OMAE2000/S&R-6120).

Rodríguez, G.R., 1993. Methods of spectral analysis (in Spanish), Report of collaboration agreement, CEDEX-ULPGC-FULP.

Rodríguez, G.R., 1995. Analysis of wind-generating gravity waves in deep waters (in Spanish), Ph.D. thesis, Universidad de Las Palmas de Gran Canaria (Spain).

Rodriguez, G.R., Guedes Soares, C., Machado, U., 1999. Uncertainty of the Sea state parameters resulting from the methods of spectral estimation. Ocean Engineering 26 (10), 991–1002.

Rice, S.O., 1944. Mathematical analysis of random noise. Bell System Technical Journal 24, 288–332.

Seemann, J., Ziemer, F., Senet, C.M., 1997. A method for computing calibrated ocean wave spectra from measurements with a nautical x-band radar. In: Proceedings of Oceans'98 Halifax, Canada, October 6–8, pp. 1148–1154, (vol. 2).

Senet, C.M., Seemann, J., Ziemer, F., 1997. An iterative technique to determine the near surface current velocity from time series of sea surface images. In: Proceedings of OCEANS'97, 500 Years Ocean Explorations, Halifax, Canada, October.

Young, I.R., Rosenthal, W., Ziemer, F., 1985. A three-dimensional analysis of marine radar images for the determination of ocean wave directionality and surface currents. Journal of Geophysical Research 90, 1049–1059.